*Available online at http://www.journalcra.com*

*International Journal of Current Research*
*Vol. 9, Issue, 03, pp.47654-47665, March, 2017*

**INTERNATIONAL JOURNAL OF CURRENT RESEARCH**

**ISSN: 0975-833X**

## RESEARCH ARTICLE

# GEOCHEMISTRY, PETROGENESIS AND METALLOGENESIS OF THE WADI QUTABAH GABBROIC INTRUSION AND ASSOCIATED NI-CU DEPOSITS, NORTH WEST YEMEN

**[1]Ali M. Al-Hawbani, [2]Khaled M. Al-Selwi, [3]Ali M. Qaid and [4,5,*]Saleh S. Albani**

[1]Department of Geology and Environmental Sciences, Faculty of Applied Sciences, Thamar University, Yemen
[2]Department of Earth and Environmental Sciences, Faculty of Science, Sana'a University, Yemen
[3]Al-Hajar (Qabitah) Community College – Lahj
[4]Department of Geology, Faculty of Oil and Minerals, Aden University- Yemen
[5]Department of Geology, Dr. Babasaheb Ambedkar Marathwada University, Aurangabad, India

**ARTICLE INFO**

*Article History:*
Received 20th December, 2016
Received in revised form
24th January, 2017
Accepted 19th February, 2017
Published online 31st March, 2017

*Key words:*

Wadi Qutabah,
Gabbroic Intrusion,
Magmatic Ni-Cu Deposit,
Northwest Yemen Geochemistry.

**ABSTRACT**

The Wadi Qutabah gabbroic intrusion associated with magmatic Ni-Cu sulfide deposit is located in the northwest of Yemen, about 60 km. of Sana'a City. Petrographic examination shows the gabbroic rocks are composed mainly of plagioclase, clinopyroxene orthopyroxene and hornblende. Two main types of sulfide mineralization have been recognized within gabbroic rocks; disseminated and massive sulfides. The principal ore minerals are pyrrhotite, pentlandite, chalcopyrite and magnetite. The chemical compositions of the gabbroic rocks represent SiO2 (47.68 - 53.13 wt. %), MgO (1.97 - 9.98 wt. %) $Al_2O_3$ (16.57 - 26.76 wt. %), $Fe_2O_3$ (2.0 - 13.35 wt. %) and $TiO_2$ (0.54 - 3.07 wt. %). The results of chemical analysis of the sulfides represent Ni (0.40 – 1.54 wt. %), Cu (0.06 – 2.46 wt. %) and Co (0.08 – 0.180 wt. %). The Wadi Qutabah gabbroic intrusion is enriched in light rare earth elements (LREE) relative to heavy rare earth elements (HREE), and exhibit positive Nb, Ta and Ti anomalies and negative Zr and Hf anomalies. Major oxide, trace element and REE data are suggestive of oceanic island evolved basalt as the parent for these gabbros. The mineralogy and tectonic discrimination diagrams suggest within plate basalt tholeiitic.



**Citation: Ali M. Al-Hawbani, Khaled M. Al-Selwi, Ali M. Qaid and Saleh S. Albani, 2017.** "Geochemistry, Petrogenesis and Metallogenesis of the Wadi Qutabah Gabbroic Intrusion and Associated Ni-Cu Deposits, North West Yemen", *International Journal of Current Research*, 9, (03), 47654-47665.

## INTRODUCTION

Wadi Qutabah area is located in the northern part of the same layered mafic complex that hosts the Suwar nickel-copper deposit (Figs. 1 a). It lies some 23 km north of Suwar and 60 km northwest of Sana'a. The study area is bounded by latitudes 1745916 and 1743820 N, and longitudes 0362005 and 0362594 E. At Wadi Qutabah, five iron sulfide horizons have been found within layered gabbroic rocks. These sulfide horizons are conformable with the primary layering of the gabbroic rocks and occur over area of 23 $km^2$. (Cantex, 2002). Many important metals, such as Ni, Cu, Co and PGE, are taken from magmatic sulfide deposit (Zhongli, *et al.,* 2005). Magmatic Ni-Cu sulfide deposits form as the result of segregation and concentration of droplets of liquid sulfide from mafic or ultramafic magma, and the partitioning of chalcophile elements into these from the silicate melt (William, 1979, Naldrett, 1999, Lightfoot, 2007 and Keays, *et al.,* 2010).

***Corresponding author:** [4,5,*]**Saleh S. Albani,***
[4]Department of geology, Faculty of Oil and Minerals, Aden University- Yemen.
[5]Department of Geology, Dr. Babasaheb Ambedkar Marathwada University, Aurangabad, India.

Sulfide saturation of a magma is not enough in itself to produce an ore deposit. The appropriate physical environment is required so that the sulfide liquid mixes with enough magma to become adequately enriched in chalcophile metals, and then is concentrated in a restricted locality so that the resulting concentration is of ore grade (Naldrett, 2004). Several factors affect the Ni, Cu and PGE grade of the sulfides of the magmatic sulfide deposits, the most important of which include, concentration of these elements in the parental silicate magma, degree of sulfide segregation and immiscibility, reaction between the sulfide droplets and new pulses of mafic, and fractionation of the sulfide liquids (Arndt, 2005, Song, *et al.,* 2001 and Macheyeki, 2012). When sulfide immiscibility and segregation (a result of crustal contamination) occur relatively earlier than the crystallization of the silicates, the sulfide droplets could be concentrated at the base of the magma chamber to form massive or semi-massive ores. In contrast, if sulfide segregation and silicate crystallization occur at the same time, they would settle down together and form disseminated sulfide ores (Hoatson, *et al.,* 2006, Schulz, *et al.,* 2010 and Song, *et al.,* 2011). This study aims at examining the petrography to consider its minerals, and geochemical properties of the gabbroic rocks to determine major element,

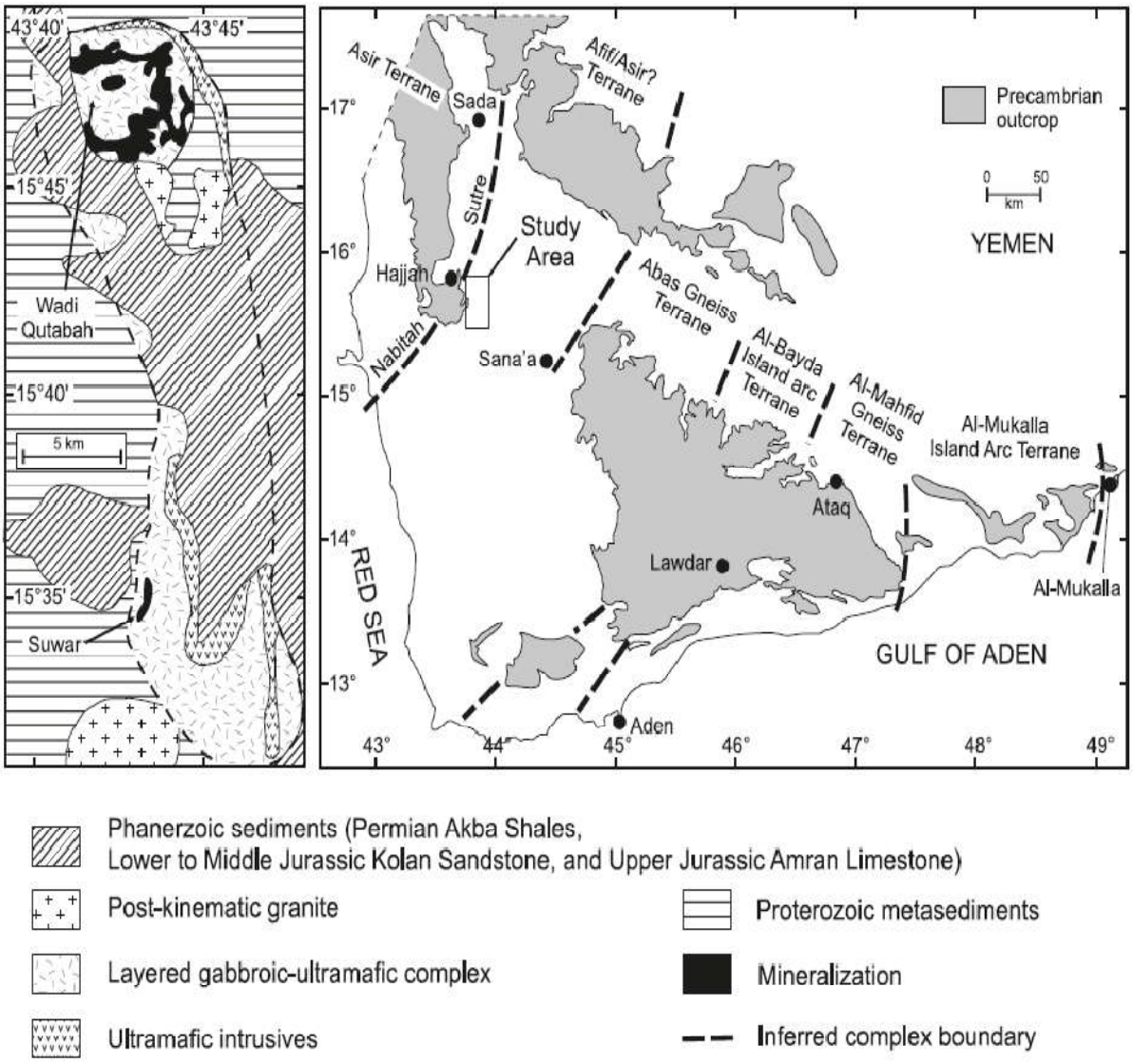


**Figure 1. Sketch map showing the geology of a) Wadi Qutabah and Suwar b) Pan-African terrane boundaries and Precambrian outcrops in Yemen. a) Unpublished map from Cantex Mine Development shows the intrusion boundary; b) map was modified from Windley et al. (1996) With additional information from Whitehouse et al. (2001)**

trace and REE elements. These are used to unravel the magmatic evolution of the gabbroic intrusion. Also to study sulfide ore to define their economic potential.

## METHODOLOGY

The methods of this study include the field work and the laboratory analyses. Eighteen rock samples were collected from the Wadi Qutabah gabbroic rocks, based on careful petrographic observation, eight fresh representative samples were chosen for major oxides, traces and rare earth elements. Major oxides were determined by X-ray fluorescence spectrometer (XRFS) techniques on a Philips PW 2400 automated spectrometer. Other trace elements, including rare earth elements (REE), were analyzed by inductively coupled plasma mass spectrometry (ICP - MS). Ten rock samples were systematically selected from the study area and thin sections which were prepared following the procedure listed in (Tucker, 1988). Eight samples were collected from the sulfide ore bodies, to make polished sections. Also_five samples were collected from the sulfide ore, samples were analyzed by inductively coupled plasma mass spectrometry (ICP- MS). The analyses were carried out at the laboratories of Al-Amri in Saudia Arabia, and in the laboratories of Geological Survey and Minerals Resources Board (GSMR) Sana'a, Yemen.

### Geological Setting

The Precambrian basement rocks of northern Yemen are late Proterozoic in age and they consist the north to northwest trending belts and composed of metavolcanic and metasedimentary rocks, intruded by granitic and gabbroic plutons. The gabbroic rocks are often layered and represent oceanic island arcs (Cantex, 2002). The Precambrian basement of the northwestern part of Yemen is an extension of the Arabian shield to the north and is petrogenetically similar to accreted oceanic arc terrains constituting the Nabitah orogenic mobile belt (Cantex, 2002 and Shybani, 2003). The Nabitah suture zone may extend to Hajjah in northwest Yemen, as indicated by the presence of dismembered deformed ophiolites (Cantex, 2002). The Precambrian rocks of study area overlapped uncomfortably by relatively thin sequences of continental to epicontinental sediments. The flat lying Paleozoic and Jurassic sediments, which cover much of the northern part of the area, include the Permian Akbara shale, which consist, mainly of shale and siltstone. The Jurassic sediments composed of the Kohlan sandstone, and upper Jurassic Amran limestone (Kruck and Schaffer, 1991). Large parts of the Northwest Yemen are overlain by volcanic rocks commonly known as the Yemen volcanic.

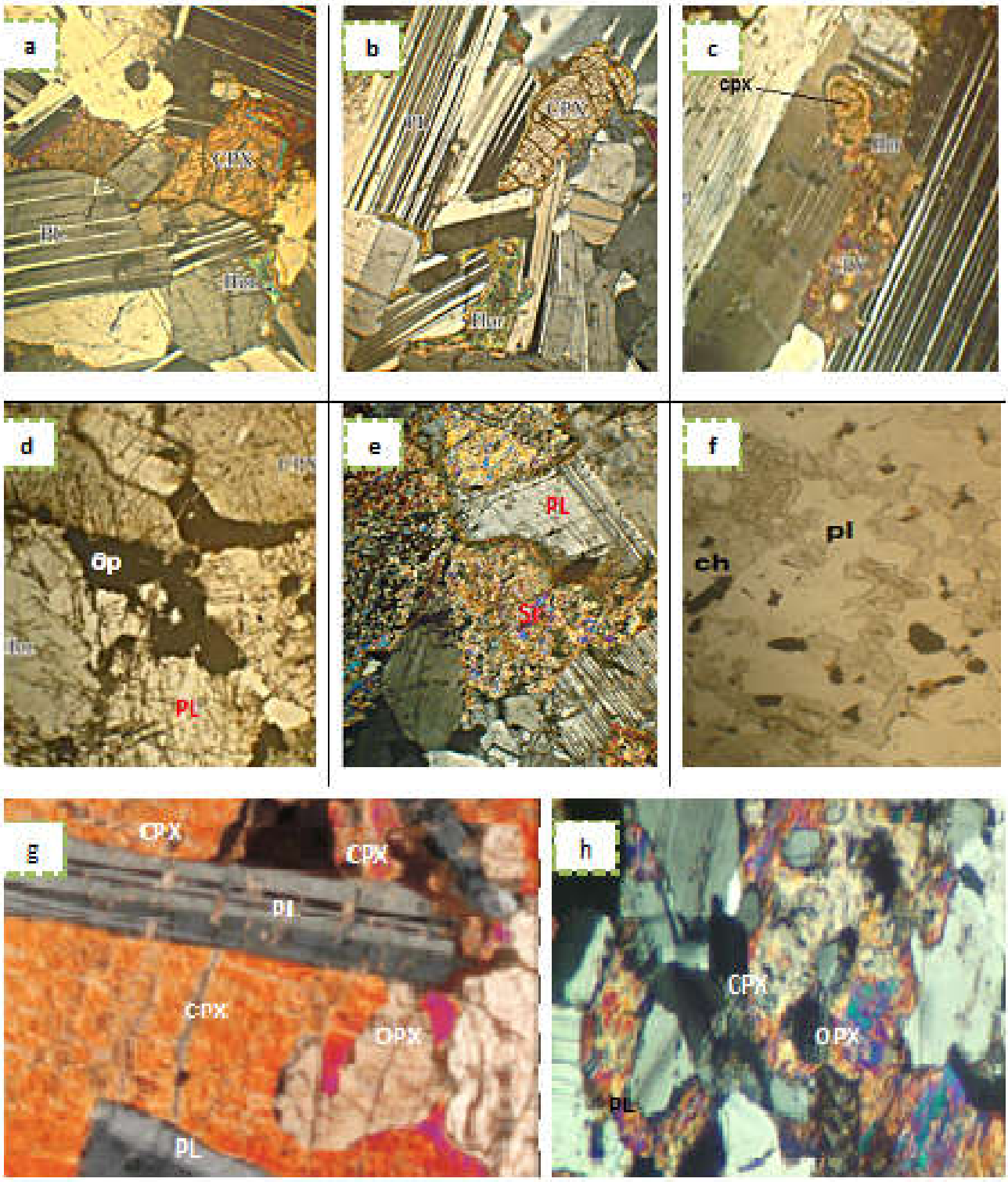


**Figure 2. Microphotographs of samples from the Wadi Qutabah gabbroic intrusion, NW. Yemen show: (a) Subhedral to euhedral plagioclase (PL), subhedral clinopyroxene (CPX), with anhedral hornblede (Hor) (CN.-40X. (b) Euhedral and subhedral plagioclase (PL), subhedral clinopyroxene (CPX) with anhedral hornblende (Hor) CN. - 40X. (c) Euhedral plagioclase (PL), subherdal to anhedral clinopyroxene (CPX), which is rimmed by hornblende (Hor) CN. - 40X. (d) Plagioclase (PL), clinopyroxene (CPX), hornblende (Hor) and opaque minerals (Op) PP. - 40X. (e) Plagioclase (PL) and altered plagioclase to sericite (Sr) CN. - 40X. (f) Plagioclase (PL) and altered clinopyroxene to chlorite (ch) PP. - 40X. (g) Large poikilitic clinopyroxene (CPX) cumulus plagioclase (PL) and orthopyroxene (OPY) CN. - 40X. (h) The finer grained, somewhat equigranular texture, plagioclase (PL), clinopyroxene (CPX) and opaque minerals (Op) CN. - 40X**

The intrusion occurs at the westerly edge of the gneissic Afif / Asir terrain (Fig. 1 b) one of six northeast-southwest oriented, arc gneiss terrains associated with Pan-African orogenesis (Windley, *et al.,* 1996, Whitehouse, *et al.,* 1998, 2001 and Greenough**,** *et al.,* 2011). The Afif terrain in Yemen mostly consists of undated orthogneisses and volcanic rocks (pillow basalt, andesite, and rhyolite) of arc origin **(**Windley, *et al.,* 1996 and Whitehouse, *et al.,* 1998, 2001). The Wadi Qutabah complex intrude a basement of meta-sediment and meta-volcanic rocks, and intruded by post-tectonic granites, pegmatitic and mafic dykes. The complex is a circular area of approximately 32 km. (Cantex, 2002 and Shybani, 2003). In addition, small mineralized outcrop occurs 4 km. south of the main body.

**Table 1. Major (wt. %) and trace element (ppm) analyses of the Wadi Qutaba gabbroic intrusion**

| *Sample No.* | *SRQ-1* | *SRQ-2* | *SRQ3* | *SRQ-4* | *SRQ-5* | *SRQ-6* | *SRQ-7* | *SRQ-8* |
|---|---|---|---|---|---|---|---|---|
| | | | | | | | *Major elements (wt. %)* | |
| $SiO_2$ | 53.13 | 49.81 | 48.57 | 52.26 | 47.68 | 51.21 | 50.92 | 48.74 |
| $TiO_2$ | 0.69 | 1.27 | 1.9 | 0.65 | 1.6 | 0.54 | 0.7 | 3.07 |
| $Al_2O_3$ | 26.76 | 23.8 | 17.67 | 23.84 | 16.57 | 19.2 | 18.13 | 16.59 |
| $Fe_2O_3$ | 2 | 11.62 0 | 13.35 | 3.02 | 11.53 | 4.96 | 6.93 | 11.6 |
| MnO | 0.04 | 0.03 | 0.17 | 0.06 | 0.14 | 0.1 | 0.12 | 0.17 |
| MgO | 1.97 | 4.51 | 6.18 | 4 | 9.98 | 8.53 | 7.94 | 7.51 |
| CaO | 10.38 | 2.32 | 7.17 | 8.55 | 8.08 | 11.61 | 11.5 | 8.33 |
| $Na_2O$ | 3.8 | 3.23 | 3.24 | 3.75 | 3.37 | 2.95 | 2.68 | 3.29 |
| $K_2O$ | 0.45 | 0.41 | 0.31 | 1.02 | 0.25 | 0.3 | 0.49 | 0.25 |
| $P_2O_5$ | 0.06 | 0.14 | 0.01 | 0.02 | 0.04 | 0.05 | 0.02 | 0.03 |
| L.O.I. | 0.4 | 2.46 | 1.32 | 2.04 | 0.7 | 0.73 | 92 | 0.1 |
| Total | 99.68 | 99.6 | 99.89 | 99.21 | 99.94 | 100.18 | 100.35 | 99.68 |
| | | | | *Trace elements ( ppm)* | | | | |
| Rb | 2.3 | 7.5 | 1.8 | 1.8 | 0.7 | 2.2 | 3.5 | 1.8 |
| Sr | 821 | 637 | 516 | 733 | 237 | 735 | 714 | 534 |
| Ba | 100 | 80 | 80 | 120 | 213 | 83 | 93 | 86 |
| Zn | 28 | 42 | 65 | 29 | 94.25 | 45 | 46 | 27 |
| Cu | 160 | 76.5 | 70.6 | 51.1 | 13.22 | 104 | 150 | 12.5 |
| Ni | 26.5 | 41.6 | 64.7 | 21 | 310 | 160 | 146 | 13 |
| Co | 25 | 13.9 | 48.4 | 80 | 37.67 | 31 | 33 | 39 |
| V | 42 | 101 | 247 | 74 | 100 | 61 | 91 | 612 |
| Cr | 118 | 46 | 94 | 74 | 180 | 167 | 100 | 41 |
| Zr | 14.1 | 2 | 2.5 | 2.2 | 10.18 | 10 | 5 | 17 |
| Y | 3.2 | 2.2 | 2.5 | 2 | 6 | 4 | 3.5 | 5.3 |
| Nb | 1.8 | 1.2 | 1.7 | 3.9 | 2.07 | 3.3 | 2.3 | 5.3 |
| Ta | 0.13 | 0.09 | 0.17 | 0.08 | 0.2 | 0.1 | 0.3 | 0.5 |
| U | 0.1 | 0.2 | 0.01 | 0.01 | 0.03 | 0.02 | 0.1 | 0.02 |
| Th | 0.2 | 0.02 | 0.02 | 0.02 | 0.12 | 0.02 | 0.1 | 0.1 |
| Hf | 0.4 | 0.1 | 0.1 | 0.1 | 0.2 | 0.3 | 0.2 | 0.4 |

L.O.I = Lost Of Ignition

**Table 2. Rare Earth Elements abundances (ppm) for representative sample from Wadi Qutabah gabbroic Intrusion**

| *Sample No.* | *SRQ-1* | *SRQ-2* | *SRQ-3* | *SRQ-4* | *SRQ-5* | *SRQ-6* | *SRQ-7* | *SRQ-8* |
|---|---|---|---|---|---|---|---|---|
| La | 2.00 | 1.20 | 0.60 | 1.20 | 2.02 | 3.10 | 2.00 | 2.10 |
| Ce | 5.37 | 2.61 | 1.12 | 2.99 | 5.50 | 7.00 | 4.40 | 4.60 |
| Pr | 0.68 | 0.31 | 0.13 | 0.37 | 0.25 | 0.88 | 0.65 | 0.63 |
| Nd | 2.90 | 1.30 | 0.60 | 1.50 | 1.20 | 4.00 | 2.70 | 2.90 |
| Sm | 0.65 | 0.32 | 0.18 | 0.34 | 0.36 | 0.86 | 0.77 | 0.77 |
| Eu | 0.84 | 0.99 | 1.77 | 1.25 | 1.34 | 0.75 | 1.30 | 1.35 |
| Gd | 0.68 | 0.35 | 0.22 | 0.36 | 0.42 | 0.86 | 0.91 | 0.72 |
| Tb | 0.12 | 0.06 | 0.05 | 0.06 | 0.05 | 0.15 | 0.15 | 0.12 |
| Dy | 0.63 | 0.35 | 0.30 | 0.36 | 0.31 | 0.92 | 0.96 | 0.56 |
| Ho | 0.14 | 0.08 | 0.07 | 0.08 | 0.06 | 0.18 | 0.19 | 0.15 |
| Er | 0.37 | 0.21 | 0.24 | 0.24 | 0.25 | 0.51 | 0.52 | 0.32 |
| Tm | 0.05 | 0.03 | 0.04 | 0.04 | 0.02 | 0.08 | 0.08 | 0.07 |
| Yb | 0.34 | 0.19 | 0.27 | 0.23 | 0.26 | 0.56 | 0.59 | 0.39 |
| Lu | 0.06 | 0.03 | 0.05 | 0.04 | 0.03 | 0.08 | 0.08 | 0.06 |

**Table 3. Chemical analysis data of sulfide ore samples from Wadi Qutabah.**

| Sample No. | SOQ1 | SOQ2 | SOQ3 | SOQ4 | SOQ5 |
|---|---|---|---|---|---|
| Ni | 0.412 | 0.641 | 0.429 | 1.54 | 0.40 |
| Cu | 0.861 | 0.112 | 0.230 | 0.06 | 2.46 |
| Co | 0.149 | 0.152 | 0.128 | 0.180 | 0.08 |

**Table 4. Trace element ratios of the Wadi Qutabah intrusion rocks**

| | *Nb/U* | *La/Nb* |
|---|---|---|
| *Wadi Qutabah intrusion* | 43.8 | 0.8 |
| *Primitive mantle* | 33.95 | 0.96 |
| *N-MORB* | 49.57 | 1.07 |
| *OIB* | 47.06 | 0.77 |
| *Average crust* | 8.45 | 1.55 |

Data Sources: data the primitive mantle, N-MORB and OIB are from (Sun and McDonough, 1989), the data of the average crust of Pettigrew, et al., (2006) and Deng, et al., (2015).

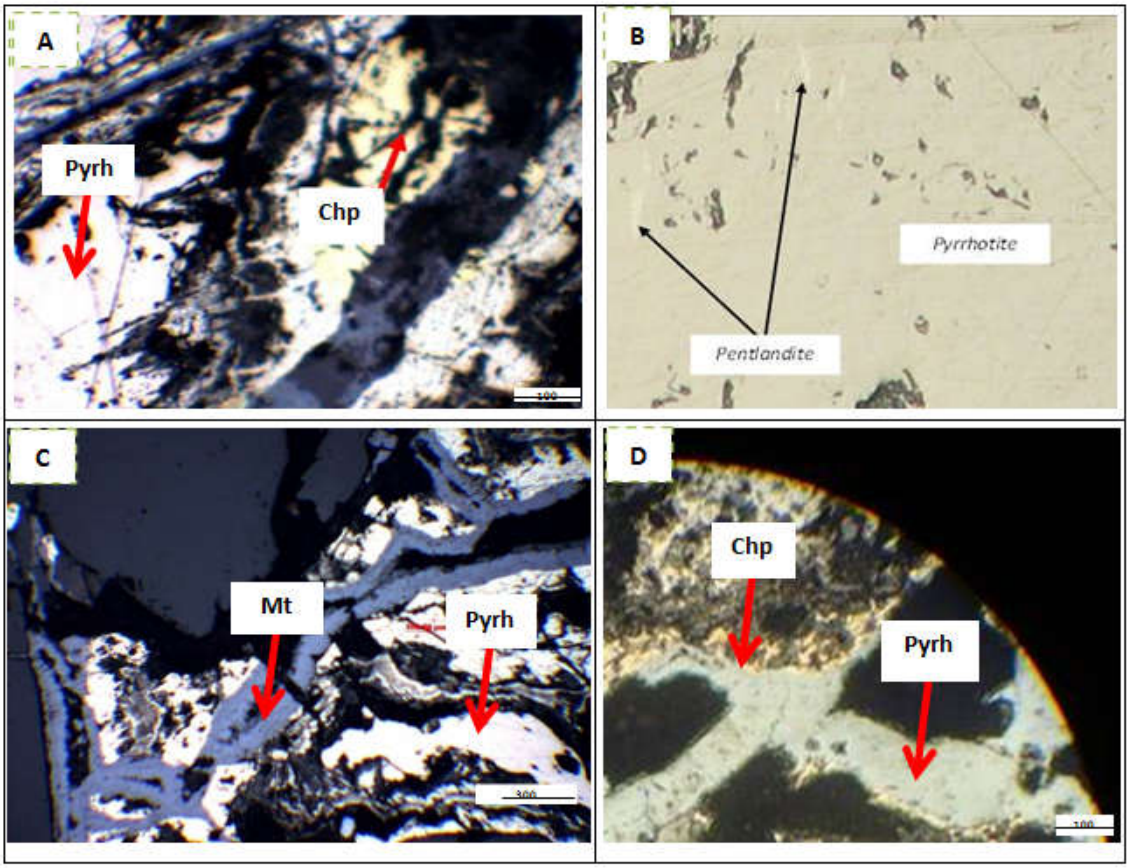


**Figure 3. Photomicrographs showing typical textures of sulfides from the Wadi Qutabah intrusion , pyrh - pyrrhotite, chp – chalcopyrite, pent – pentlandite, Mt - magnetite: (a) Anhedral chalcopyrite intergrown with pyrrhotite. (b) Pentlandite exsolution flame in pyrrhotite. (c) Anhedral pyrrhotite intergrown with magnetite. (d) Chalcopyrite as irregular grains along the margins of pyrrhotite. In reflected light, plane polarized light. b and c photographs are 300 µ. Wide, a and d photographs are 100 µ Wide**

The Wadi Qutabah complex consist three major units of gabbro, gabbro - norite, and discontinuous ultramafic lens.
Five main mineralized horizons have been discovered within Wadi Qutabah complex. These iron sulphide horizons are conformable with the primary layering of gabbroic body and occur over an area of 23 $km^2$ (Cantex, 2002). The sulfide horizons outcrop mainly as disseminated and massive gossans but fresh sulfides are exposed in steep narrow gullies where the gossans have been eroded. The widely distributed white rocks through the eastern part of the complex are pegmatitic dykes and sills. Several faults can be seen cross-cutting the Wadi Qutabah complex, categorized into older normal faults, strike slip faults, and younger normal faults.

## Petrography

The gabbro is composed of plagioclase (30% - 70%), clinopyroxene (10% - 35%), orthopyroxene (0% - 15%), hornblende and opaque minerals 5% - 25%, (Fig. 2a,b). Plagioclase is present as almost euhedral perfect crystals range in size from 0.5 up to 5 mm, the polysynthetic twinning is one of plagioclase's very common features (Fig. 2b & c). Clinoproxene forms subhedral and anhedral grains, reaching up to 4 mm in size. Hornblende is presented anhedral to subhedral crystal. The hornblende is intergrown with or enclosed in clinopyroxene. Some plagioclase is surrounded by hornblende (Fig. 2a & b). Poikilitic textures can be observed in large clinopyroxene crystal which includes numerous inclusions of plagioclase and orthopyroxene (Fig. 2g). Orthopyroxene forms anhedral and subhedral (Fig. 2g).

Most clinopyroxene are surrounded by hornblende (Fig. 2 a, b & c). Clinopyroxene are rimmed by hornblende, suggesting reaction between the hydrous oxide melt and silicate minerals (Fig. 2a,c). Sometimes plagioclase alters to sericite (Fig. 2e). Clinopyroxene is altered to chlorite (Fig. 2f). Textures imply crystallization of plagioclase, orthopyroxene, clinopyroxene and hornblende in that order.

## Sulfide Mineralogy

Ore minerals include pyrrhotite, pentlandite, chalcopyrite and magnetite. The main sulfide minerals observed in the disseminated and massive sulfide mineralization. Pyrrhotite is the dominant sulfide mineral in all the sulfide ores. It occurs mainly as anhedral or subhedral crystals with grain size from 0.1 to 3.0 mm. (Fig. 3a & b). Pyrrhotites occur as intergrowths with chalcopyrite and magnetite (Fig. 3a & c). Pentlandie is closely associated with pyrrhotite and commonly occurs as exsolution flames in pyrrhotite grains, or along fractures within pyrrhotite (Fig. 3b). Chalcopyrite occurs predominantly as anhedral grains or irregular grains along the margins of pyrrhotite crystals (Fig. 3a & d). Magnetite occurs as veins cutting through pyrrhotite and chalcopyrite crystals (Fig. 3c).

## Geochemistry

Chemical analysis was carried out for eight selected rock samples of the gabbroic intrusion and five selected sulfide ore samples for (Ni, Cu, Co). The analyses were carried out at the laboratories of Al-Amri in Saudia Arabia, and in the laboratories of Geological Survey and Minerals Resources Board - Sana'a /Yemen.

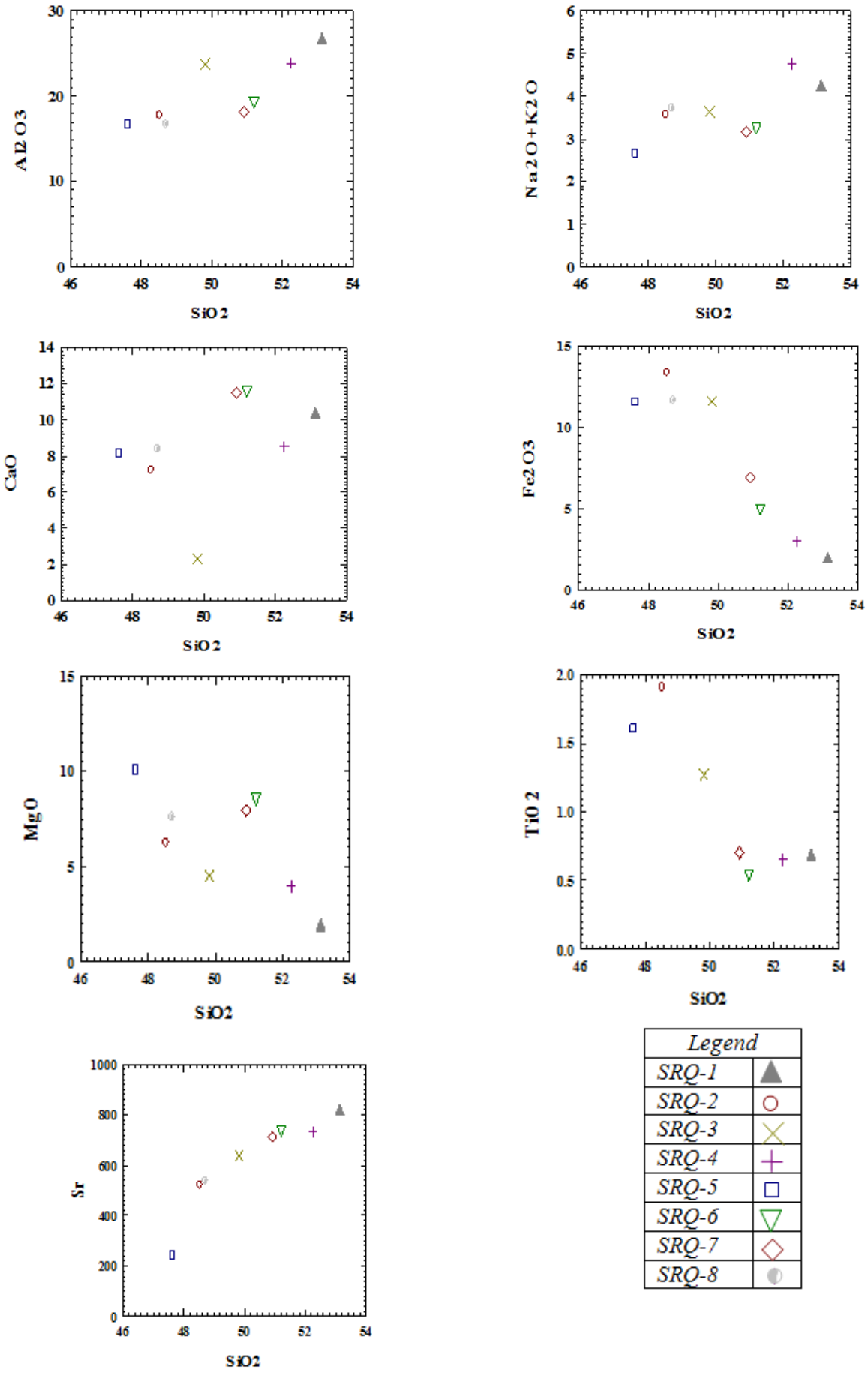


**Figure 4. $SiO_2$ vs. $Al_2O_3$, $Na_2O + K_2O$, CaO, $Fe_2O_3$, MgO, $TiO_2$ and Sr for rocks of the Wadi Qutaba intrusion Yemen**

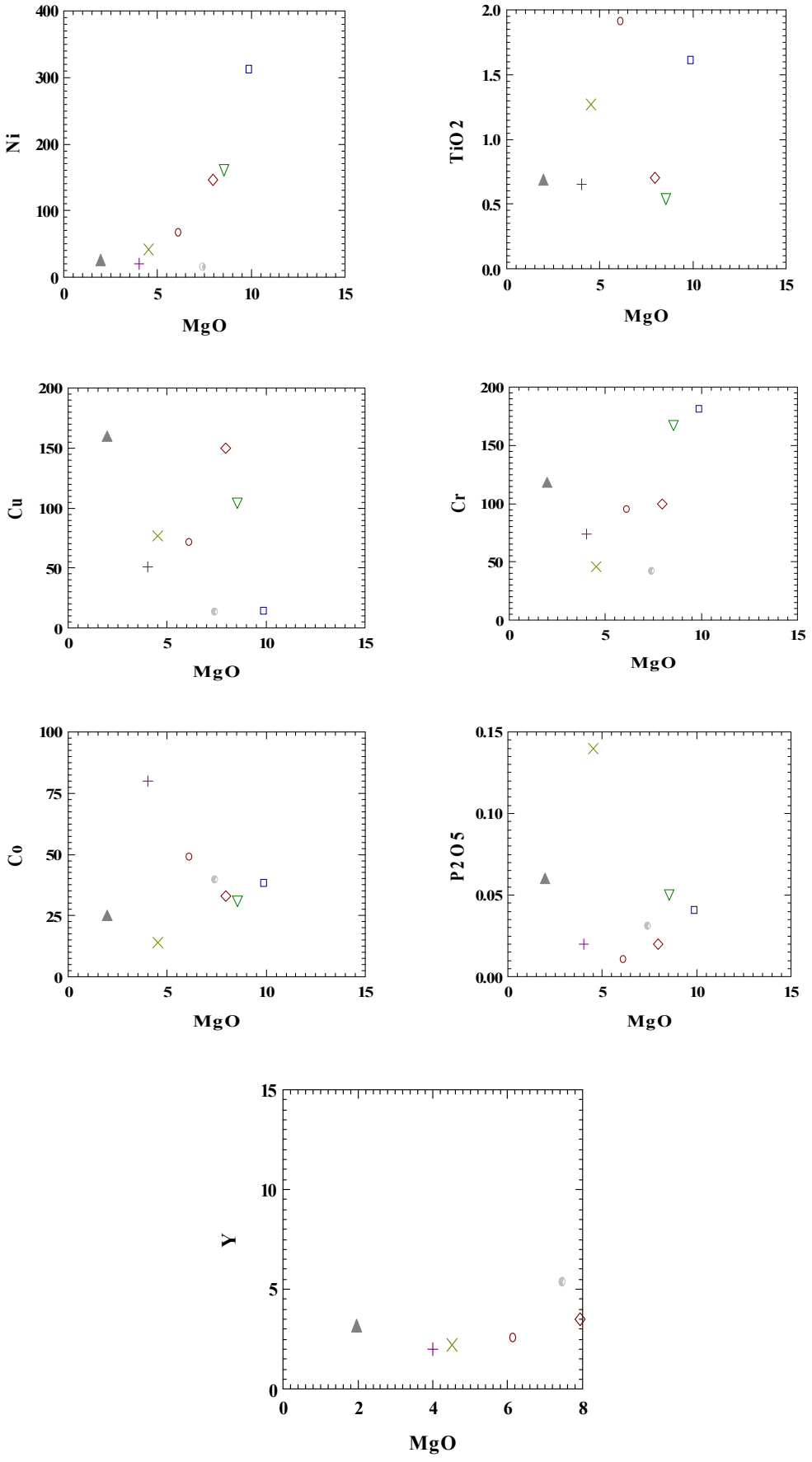


**Figure 5. The MgO vs. $TiO_2$, Ni, Cu, Cr, Co, $P_2O_5$, and Y for rocks of the Wadi Qutabah intrusion, symbols as in (Fig. 5)**

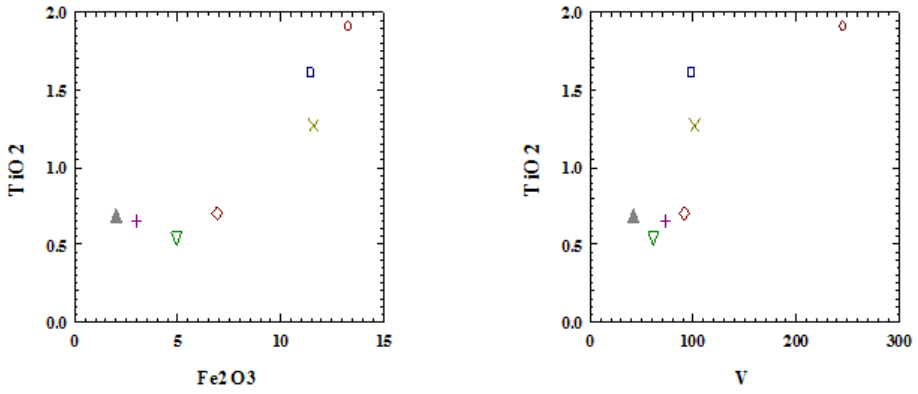


**Figure 6. $TiO_2$ vs. $Fe_2O_3$ as (total iron) and V in the Wadi Qutabah intrusion, symbols as in (Fig. 8)**

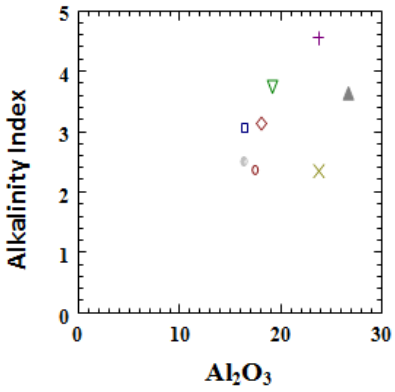


**Figure 7. Alkalinity index vs. $Al_2O_3$ in Wadi Qutabah intrusion, Yemen, symbols as in (Fig. 8)**

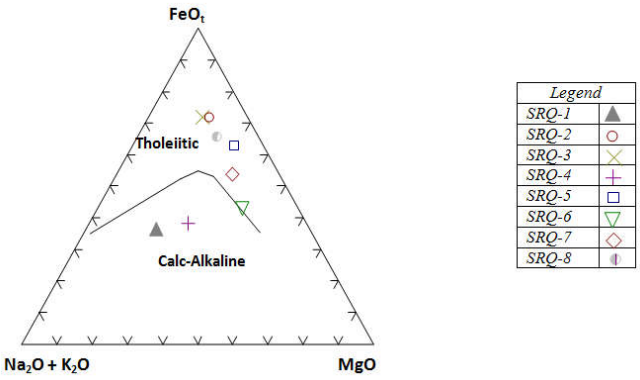


**Figure 8. Atomic Force Microscopy diagram showing geochemical variations in the Wadi Qutabah intrusion NW Yemen. Tholeiitic and Calc-Alkaline trends are after Wilson (1989)**

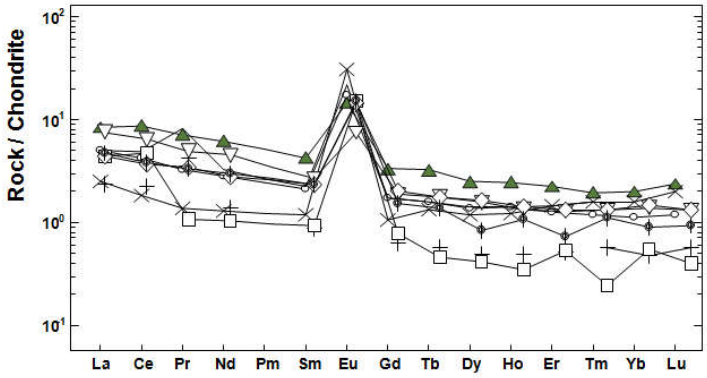


**Figure 9. Chondrite-normalized rare earth elements diagram for Wadi Qutabah intrusion. Chondrite normalizing values of Sun and McDonough, (1989) Symbols as in (Fig. 8)**

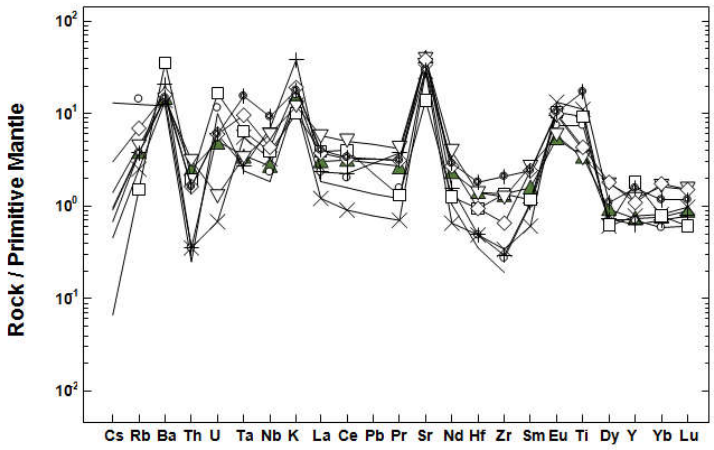


**Figure 10. Primitive mantle normalized trace element diagram of the Wadi Qutabah gabbroic intrusion. Primitive mantle normalization value are from (McDonough and Sun, 1995), Symbols as in (Fig. 8)**

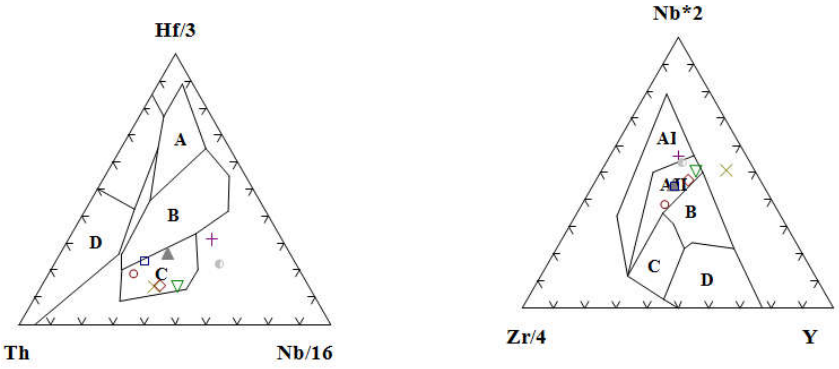


A = N- type MORB
B = E- type MORB & WPT
C = Alkaline within plate basalt
D = Island arc tholeiite

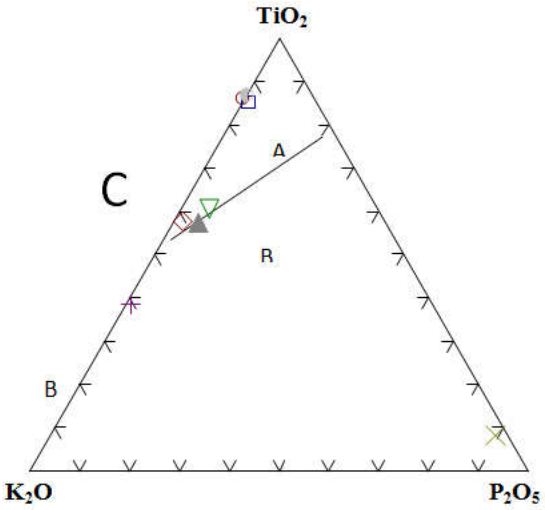


**Figure 11. Element-ratio –based on discrimination diagrams showing Wadi Qutabah samples. Diagram source are A- after Wood, *et al.,* (1980). B- after Mesched, (1986). C- after Pearce, *et al.,* (1975) Symbols as in (Fig. 8)**

## Major Elements

Table (1) shows chemical analyses of representative samples from Wadi Qutaba gabbroic intrusion. The results of chemical analyses of representative samples from Wadi Qutaba gabbroic intrusion indicated that concentration silica oxide is variegated from 47.69 wt. % to 53.13 wt. % and $Al_2O_3$ content from 16.57 wt. % to 26.76 wt. % . $Na_2O$ and $K_2O$ range from 2.68 to 3.80 wt. % and from 0.25 to 1.02 wt. % respectively, whereas CaO content from 2.32 wt. % to 11.61 wt. %. The gabbros are relatively rich in $Fe_2O_3$ and $TiO_2$, ranging between 2.00 and 13.35 wt. % and 0.52 and 3.07 wt. % respectively.

There is no systematic variation of major oxides through the intrusion, although there is a slight overall decrease in $Fe_2O_3$ (as total iron) and MgO and an increase in $SiO_2$, $Na_2O$, $Al_2O_3$ (Figs. 4, 5). $Al_2O_3$ versus $SiO_2$ plots have been used based on the facts that $Al_2O_3$ is hosted in rocks rich in feldspars. $SiO_2$ is hosted in silicates (in this case, mafic rocks). The $Al_2O_3$ versus $SiO_2$ plots (Fig. 4) show two different trends and a positive correlation meaning that generally, $Al_2O_3$ content increases with increasing $SiO_2$ content. In the gabbros CaO and total alkalis ($Na_2O + K_2O$) increase with increasing $SiO_2$, and shows two slightly different trends (Fig. 4), whereas MgO, $Fe_2O_3$ and $TiO_2$ decrease. $Fe_2O_3$ (as total iron) and $TiO_2$ are clearly and positively correlated (Fig. 6). $P_2O_3$ decreases with increasing MgO, this trend is followed by Cu (Fig. 5). The very low $P_2O_3$ content (0.01- 0.14) in the gabbro suggests that this intercumulus liquid was driven out by post-accumulation crystal growth (i.e., this gabbro may have adcumulus properties as defined by Wager and Brown**,** (1968). MgO versus compatible elements: e.g. Ni and Cr (Fig. 5) exhibit the fractionation / accumulation of pyroxene, plagioclase, for example, a negative correlation of MgO with $SiO_2$, CaO, $Al_2O_3$ and $K_2O + Na_2O$ indicates the fractionation /accumulation of clinopyroxene and plagioclase, a positive correlation of MgO with $Fe_2O_3$ and compatible elements (e.g. Cr, Ni and Co) is consist with fractionation / accumulation of pyroxene. The Atomic Force Microscopy (AFM) diagram (Wilson, 1989) indicates that these magma belong to the tholeiitic trend (see Fig. 8), also the rocks are by definition tholeiitic because they contain orthopyroxene.

The calculated major element composition of the Wadi Qutaba gabbroic intrusion is reported in Table (1). This composition is similar to the average high alumina basalt in the Abu Zawal gabbroic intrusion, Egypt (El-Ela, 1996) and high alumina basalt in the Voisey's Bay, Canada (Schulz, *et al.,* 2010).

Classification of volcanic rocks on the basis of alkalinity index as described by

(Cox, *et al.,* 1979) as following:

$$A.I = Na_2O + K_2O / ((SiO_2 - 43) \times 0.17)$$

The plot of alkalinity index vs. $Al_2O_3$ (see Fig. 7) shows that the studied rocks samples fall in the field of high alumina basalt.

**Trace Elements**

Trace element compositions of Wadi Qutabah gabbroic rocks are listed in Table (1). The concentrations of Ni, Cu, Co, Cr, V and Sr ranging from 28.5 to 422 ppm, 13.22 to 160 ppm 25 to 80 ppm, 46 to 200 ppm, 42 to 247 ppm and 237 to 821 ppm respectively.. Strontium content increases with increasing $SiO_2$ (Fig. 4), and reflects the modal abundance of plagioclase.

Yttrium increases with increasing MgO, this behavior is also followed by Ni and Cr (Fig. 5). Vanadiumisstrongly partitioned into titan magnetite and shows a positive correlation with $TiO_2$ (Fig. 5) The gabbroic rocks are enriched in light rare earth elements (LREE) relative to heavy rare earth elements (HREE) and show positive Eu anomalies (Fig. 9). The positive Eu anomaly in the gabbro is due to preferential Eu incorporation by the first accumulating plagioclase. The variations in the scale of the Eu anomaly in the gabbros are ascribed to a combination of the degree of Eu fractionation in the magma and the amount of cumulus plagioclase present in the taken samples. Trace element characteristics, namely , the positive Nb, Ta and Ti anomalies and negative U, Th, Zr, Y and Hf anomalies (Fig. 10) similar to oceanic island and mid-ridge basalts (Hofmann, 1986, 1988, Zou, *et al.,* 2000). Wadi Qutabah samples exhibit positive Sr, and Ba anomalies and low Rb relative to Ba (Fig. 10). The results of chemical analysis of representative sulfide samples from Wadi Qutabah indicated that concentration as; Ni (0.40 – 1.54 wt. %), Cu (0.06 – 2.46 wt. %) and Co (0.08 – 0.180 wt. %).

## DISCUSSION

The concentration of MgO in the Wadi Qutab gabbroic intrusion is variegated from 1.97 to 9.98 wt. % with an average of 6.2 wt. %. The gabbroic rocks have low percentage of MgO (6 – 10 wt %), contain high grade of copper comparing to nickel like Duluth host rock in United States and Kurissk deposit in Siberian platform (Ross and Keays, 1979, Chai, *et al.,* 2008, Al-Hawbani, 2010, Ding, *et al.,* 2011, Houle, *et al.,* 2013 and Sharkov, *et al.,* 2014). But it is possible to predict an increase of Ni concentration if the MgO concentration is getting increased in lower zone. The depletion of Ni relative to Cu can be explained by fractionation of olivine, which preferentially concentrates Ni (Barnes, *et al.,* 1985, Keays, *et al.,* 1999, Zhou, *et al.,* 2005, Chai, *et al.,* 2008, Schulz, *et al.,* 2010 and Sharkov, *et al.,* 2014). These features, together with lower MgO, Co and Cr contents Table (1), lower Mg/Fe ratios in ferromagnesian mineral, lower Ca/Na ratios in plagioclase, higher concentrations of incompatible elements in Wadi Qutabah samples, and higher concentrations of $Al_2O_3$ suggest formation from a more evolved magma.

The positive Ti, Nb, Ta anomalies and negative Th, Zr and Hf anomalies in the Wadi Qutaba rocks (Fig. 11) cannot be explained by upper crustal contamination because upper crustal rocks are typically enriched in these elements and depleted in Nb, Ta and Ti (Taylor and McLennan, 1985, Zhou, 2005, Schulz, *et al.,* 2010 and ChangYi, *et al.,* 2015). The Zr/ Nb ratios in mafic rocks range from about 40 in mid-ocean ridge basalt (MORB) to 10 in E- type MORB, and to < 10 in ocean island basalt (OIB) and rift-related lavas (Pearce and Norry, 1979, Song *et al.,* 2001 and Zhou *et al.,* 2005; Keays and Lightfoot**,** 2010). The Zr/ Nb ratios of the Wadi Qutaba gabbros vary between 2 and 14 with most less than 10, similar to oceanic island basalt (OIB) (Song, *et al.,*2001). In addition, the low Zr/Y (0.8 - 1.84) observed among the gabbroic zones support an oceanic arc setting rather than a continental arc setting (Pearce, 1984 and Polyakov, 2013). The Th/U ratio of the Wadi Qutaba gabbros from 2.0 to 4.0 with an average of 3.0, comparable with ratios of 3.0 - 3.8 for OIB, but less than ratios of 4.5 - 4.9 enriched mantle-EM1 (Weaver, 1990 and Deng *et al.,* 2015). Based on the rate of Th/Nb, the tectonic setting of ocean and continent can be divided by Th/Nb = 0.11 which is similar the value of initial mantle (Wang, *et al.,* 2001, Sun, *et al.,* 2006 and Jia, *et al.,* 2013), the basaltic rocks formed within continent with Th/Nb > 0.11 and formed within ocean such as MORB and OIB with Th/Nb < 0.11. The Th/Nb ratios of the Wadi Qutabah gabbroic rocks have < 0.11, similar to the source for ocean island basalt. Compared with the average crust, N-MORB, ocean island basalt (OIB) and primitive mantle, the Wadi Qutabah intrusion has higher Nb/U ratio and lower La/Nb ratio Table (4). These trace elements ratios cannot be formed by the contamination of the mantle end-member with the crust but reflect the feature of the mantle of the Wadi

Qutabah intrusion. The Nb/U and La/Nb ratios of the Wadi Qutaba intrusive rocks are similar to oceanic island basalt, suggesting that the primary magma of the intrusion was derived from a mantle source. The discrimination diagrams employing incompatible element ratios might provide information on the character of original magma. Average La/Yb is 4.4 in Wadi Qutabah (La/Yb in tholeiites = 3.5 - 9.6) Greenough, *et al.,* (2005). In Hf/3-Nb/16 –Th ternary discrimination diagram (Wood, *et al.,* 1980) shows most samples are falling in the field C within plate basalt. Anomalous Nb nudged samples SRQ-4 and SRQ-8 toward the Nb apex (Fig. 11A) and plot just outside of the within- plate- basalt field. High Nb shifted these samples away from the Hf and Th. In Nb*2-Zr/4 –Y diagram (Mesched, 1986) all samples are put in the field of AII (Fig. 11B) within plate alkali and tholeiitic basalt (WPATB). In $TiO_2$ – $K_2O$ - $P_2O_3$ diagram (Pearce, *et al.,* 1975) all rocks put in the field of oceanic basalt. The three samples with high $TiO_2$ (see Table 1) plotting near the Ti apex (Fig. 11C). Considering all of the above, and all of the samples, the original magma apparently had tholeiitic, within plate basalt characteristics. Major oxide, trace element and rare earth element (REE) data in Wadi Qutabah gabbroic intrusion are suggestive of oceanic island evolved basalt as the parent for these gabbros.

**Conclusion**

The Wadi Qutabah gabbroic intrusion mainly consists of plagioclase, clinopyroxene, orthopyroxene and hornbleblende. The principal ore minerals are pyrrhotite, pentlandite, chalcopyrite and magnetite. The Wadi Qutabah gabbroic intrusion may have crystallized from an oceanic island high alumina basaltic magma, which was derived from mantle source, is suggested by the observations mentioned above. Exploration at Wadi Qutabah is at preliminary stage and these early results are regarded as encouraging. Future exploration strategies should be taken into account:

- Evaluation of the tectonic framework of the magmatic sulfide deposit.
- Estimation of the type mineralization by checking depletion of Ni, Co, and PGE of the comagmatic intrusive rocks.
- Geophysical and geochemical survey to locate large pods of sulfide.
- Planning of the drill holes in the target area based on the geochemical and geophysical anomalies.
- References

## REFERENCES


Al-Hawbani, A. M. 2010. Geological and geochemical investigation of host rocks of Ni – Cu in Suwar area north western Yemen. *Thamar University Journal of Natural and Applied Sciences.*, 2: 41- 54.

Arndt, N. T. 2005. The conduits of magmatic ore deposits. *Exploration For platinum-group element deposits: mineralogical Association of Canada Short Course Notes.*, 35: 181-201.

Barnes, S. J., Naldrett, A. J., Gorton, M. 1985. The origin of the fractionation of platinum- Group elements in terrestrial magmas. *Chemical Geology.*, 53: 303 - 323.

Cantex Mine Development Corporation – Yemen, 2002. 3rd. Annual report to the Geological Survey and Minerals Resource Board, Republic of Yemen., pp. 31

Chai, F., Zhang, Z. C., Mao, J., Dong, L., Zhang, Z. H., Wu, H. 2008. Geology, petrology and geochemistry of the Baishiquan Ni-Cu-bearing mafic-ultramafic intrusions in Xinjiang, NW China: Implication for tectonics and genesis of ores. *Journal of Asian Earth Sciences.*, 32: 218 - 235.

ChangYi, J., JinLan, L., Wei, Z., Wei, D., ZiXi, W., YaZhou, F., YanFang, S., ZhongBao, S. 2015. Petrogenesis of the Xiarihamu Nibearing layered mafic-ultramafic intrusion, East Kunlun: Implications for its extensional island arc environment. *Acta Petrologica Sinica*., 31: 1117-1136.

Cox, K. G., Bell, J. D., Pankhurst, R. J. 1979. The interpretation of igneous rocks. London, Allen and Unwin., pp. 450.

Deng, Y., Yuan, F., Zhou, T., Xu, C., Zhang, D., Guo, X. 2015. Geochemical characteristics and tectonic setting of the Tuerkubantao mafic ultramafic intrusion in West Junggar, Xinjiang, China. *Geoscience Forntiers*., 6: 141-151.

Ding, X., Ripley, E. M., Li, C. 2012. PGE geochemistry of the Eagle Ni–Cu–(PGE) deposit, Upper Michigan: constraints on ore genesis in a dynamic magma conduit. *Mineralium Deposita.*, 47: 89-104.

El-Ela, F. F. A. 1996. The petrology of the Abu Zawal gabbroic intrusion, Eastern Desert, Egypt: an example of an Island-Arc setting. *J. Afr. Earth Sci.*, 22: 147 - 157.

Greenough, J. D., Dostal, J., Mallory-Greenough, L. M. 2005. Oceanic island volcanism II: mantle processes. *Geoscince Canada*, 32: 83 - 108.

Greenough, J. D., Kamo, S. L., Theny, L., Crowe, S. A., Fipke, C. 2011. High-precision U-Pb age and geochemistry of the mineralized (Ni-Cu-Co) Suwar intrusion, Yemen. *Can. J. Earth Sci*., 48: p. 495 - 514.

Hoatson, D. M., Jaireth, S., Jaques, A. L. 2006. Nickel sulphide deposits in Australia- Characteristics, resources and potential: *Ore Geology Reviews*., 29: 177 - 241.

Hofmann, A. W. 1986. Nb in Hawaiian magmas: constraints on composition and evolution. *Chem. Geol*., 57: 17 - 30.

Hofmann, A. w. 1988. Chemical differentiation of the earth: the relationship between mantle, continental crust, and the oceanic crust. *Earth Planet. Sci. Lett*., 90: 297-314.

Houle, M. G., Lesher, C. M., Metsaranta, R. T., Goutier, D., Gilbert, H. P., McNicoll, V. 2013. Temporal and spatial distribution of magmatic Ni-Cu-PGE, Cr and Fe-Ti-V deposits in the Bird River-Uchi-Oxford-Stull-La Grande-Eastmain Superdomain: a new Metallotect within the Superior Province. *Mineral Deposit research for A High-Tech*., 3: 1009-1012.

Jia, D. C., Liu, S., Zhong, H., Feng, G., Qi, Y., Gao, W., Zhang, X., Jiang, T., Mao, Y. 2013. Tectonic setting of the Cu-Ni sulfide–bearing mafic-ultramafic complex in northern Jilin province NE-China. *International J. of Geosciences*., 4: 317-328.

Keays, R. R., Lesher, C. M., Lightfoot, P. C., Farrow, C. E. G. 1999. Dynamic Processes magmatic Ore Deposits and their application in mineral exploration. *Geological Association of Canada Short Course*., Ch. 13: pp. 477.

Keays, R. R., Lightfoot, C. P. 2010. Crystal sulfur is required to form magmatic Ni-Cu Sulphide deposit-evidence from chalcophile element signatures of Siberian and Decan trap basalt: *Mineralium Deposita*., 45: 241-257.

Kruck, W., Schaffer, U. 1991. Geological map of the Republic of Yemen, sheet, Al Hudaydah 1:250.000. Ministry of Oil and Natural Resources, Sana'a Yemen and Fedral Institute for Geosciences and Natural Resources. Hannover, Germany.

Lightfoot, P. C. 2007. Advances in Ni-Cu-PGE sulphide deposit models and implications for Exploration technologies. Plenary Session: Ore Deposits and Exploration Technology. In (Proceedings of Exploration 07: 5th Decennial International Conference on Mineral Exploration) edited by B. Milkerreit, pp. 629 - 646.

Macheyeki, A. S. 2012. Ni mineralization and PGE characterization in the Kabanga and Luhuma Ni-Cu sulfide deposits North West Tanzania, *Tanz. J. Sci*., 38: 1-27.

McDonough, W. F., Sun, S. S. 1995. The composition of the Earth. *Chem. Geol*, 120: 223 - 253.

Mesched, M. 1986. A method of discriminating between different types of mid – oceanic ridge basalts and continental tholeiites with the Nb- Zr - Y diagram. *Chem. Geol*., 56: 207- 218.

Naldrett, A. J. 1999. World-class Ni-Cu-PGE deposits: key factors in their genesis. *Mineralium Deposita*., 34: 227-240.

Naldrett, A. J. 2004. Magmatic sulfide deposits: Geology and Exploration, Springer, pp. 727.

Pearce, J. A. 1984. Role of the sub-continental lithosphere in magma genesis at active continental margins. 230 - 249.

Pearce, J. A., Gorman, B. E., Birkett, T. C. 1975. The $TiO_2$ - $K_2O$ - $P_2O_5$ diagram: a method of discriminating between oceanic and non- oceanic basalts. *Earth Planet. Sci. Lett*., 24: 419 – 426.

Pearce, J. A., Norry, M. J. 1979. Petrogenetic implications of Ti, Zr, Y, and Nb Variations in volcanic rock. *Contributions to mineralogy and petrology*., 69: 33-47.

Pettigrew, N., Hattor, K. 2006. The Quetico intrusion of western superior province: neo-archean examples of Alaskan Ural-type mafic- ultramafic intrusions. *Precambrian Research*., 149: 21-42.

Polyakov, G. V., Tolstykh, N. D., Mekhonoshin, A. S., Izokh, A. E., Podlipskii, M. Yu., Orsoev, D. A., Kolotilina, T. B. 2013. Ultramafic-mafic igneous complexes of the Precambrian east Siberian metallogenic province (southern framing of the Siberian Craton): age, composition, origin and ore potential. *Russian Geology and Geophyics*., 54: 1319 - 1331.

Ross, T. R., Keays, R. R. 1979. Precious metals in volcanic-type nickel sulfide deposits in western Australia. Relationship with the composition of the ores and their host rocks. *Canadian Mineralogist*., 17: 417 - 435.

Schulz, K. J., Chandler, V. W., Nicholson, S. W., Piatak, N., Seal, R. R., Woodruff, L. G., Zientck, M. L. 2010. Magmatic sulfide - rich nickel - copper deposits related to Picrate and (or) tholeiitic basalt dike-sill complexes: A preliminary deposit model: *U. S. Geological Survey Open File Report*., 1179: 1 - 25.

Sharkov, E. V., Chistyakov, A. V. 2014. Geological and petrological aspect of Ni-Cu mineralization in the early paleoproterozoic Monchegorsk layered mafic-ultramafic complex, Kola Peninsula. *Geology of the ore deposits*., 56: 147-168.

Shaybani, A. M. 2003. Works and results of Canadian Mountain, activities in the northwest of Yemen, the eight Arab Conferences on Mineral resources, Sana'a Republic of Yemen, pp. 205 - 218.

Song, X. Y., Wang, Y. L., Chen, L. 2011. Magmatic Ni-Cu (PGE) deposits in magma plumbing systems: features, formation and exploration. *Geoscience Frontiers*., 2: 375 - 384.

Song, X. Y., Zhou, M. F., Hou, Z. Q., Cao, Z., Wang, Y., Li, Y. 2001. Geochemical constraints on the mantle source of the upper Permian Emeishan continental flood basalt, southwestern China. *International Geology Review*., 43: 213-225.

Sun, S. Q., Zhang, C. J. Huang, R. Q. 2006. The tectonic setting discrimination of the basalt in the convergent margin of plate by Th, Nb and Zr. *Advances in Earth Science*, 21: 593-598.

Sun, S. S., McDonough, W. 1989. Chemical and isotopic systematics of oceanic basalts: implications for mantle composition and processes. *Geological Society London Special Publication*., 42: 313 - 345.

Taylor, S. R., McLennan, S. M. 1985. The Continental Crust: its composition and Evolution. Oxford: Blackwell, pp. 312.

Tucker, M. E. 1988. Technique in sedimentology. Black Well Scientific Publication: 394p.

Wager, L. R., Brown, G. M. 1968. Layered igneous rocks.W. H. Freeman and Company. 588pp.

Wang, Y. L., Zhang, C. J., Xiu, S. Z. 2001. Th/Hf - Ta/Hf Identification of Tectonic Setting of Basalts. *Acta Petrologica Sinica*., 17: 413 - 421.

Weaver, B. I. 1990. Geochemistry of high-undersaturated ocean island basalt suites from the south Atlanti Oceanic: Fernando de Noronha and Trinidade Island basalt. *Contribution to Mineralogy and Petrology*., 105: 502 - 515.

Whitehouse, M. J., Windley, B. F., Ba-Bttat, M. A. O., Fanning, C. M., Rex, D. C. 1998. Crustal evolution and terrin correlation in the eastern Arabian shield, Yemen: geochronological constrain. *Journal of the Geological Society*., 155: 281 - 295.

Whitehouse, M. J., Windley, B. F., Stoeser, D. B., Al-Khirbash, S., Ba-Bttat, M. A. O., Haider, A. 2001. Precambrian basement character of Yemen and correlastions with Saudi Arabia and Somalia. *Precambrian Research*, 105: 357 - 369.

William, D. A. C. 1979. The association of some nickel sulfide deposits with komatiitic volcanism in Rhodesia. *Canadian Mineralogist*., 17: 337-349.

Wilson, W. 1989. Igneous petrognesis: A Global Tectonic Approach. London: Unwin Hyman, 494p.

Windley, B. F., Whitehouse, M. J., Ba-Bttat, M. A. O. 1996. Early Precambrian gneiss terrains and Pan-African island arcs in Yemen: crustal accretion of the eastern Arabia shield. *Geology*, 24: 131-134.

Wood, D. A. 1980. The Application of Th-Hf-Ta diagram in problems of tectonomagmatic classification and to establishing the nature of crustal contamination of basaltic lavas of the British Tertiary volcanic province. *Earth planet Sci. Lett*., 50, 11-30.

Zhongli, T., Haiqing, Y., Jiangang, J., & Xiaohu, L. 2005. New classification of magmatic sulphide deposits in China and metallogenesis related to small intrusions. In *Mineral Deposit Research: Meeting the Global Challenge*. pp. 57-59. Springer Berlin Heidelberg.

Zhou, M. F., Robinson, P. T., Lesher, C. M., Keays,R. R., Zhang, C. J., Malpas, J. 2005. Geochemistry, petrogenesis and Metallogenesis of the Panzhihua gabbroic layered Intrusion and associated Fe-Ti - V oxide deposits, Sichuan Province, SW China. *Journal of Petrology*., 46: 2253 - 2280.

Zou, H., Zindler, A., Xu, X.S., Qi, U. 2000. Major, trace element, and Nd, Sr and Pb isotope studies of Cenozoic basalt in SE China: mantle source, regional variations and tectonic significance. *Chemical Geology*, 171: 33 - 47.

*******